Chapter 18
Study of the Dynamic Properties of Reinforced Concrete Under High-Speed Compression

Mikhail E. Gonov, Vladimir V. Balandin, Anatoly M. Bragov, and Aleksandr Yu. Konstantinov

Abstract An experimental study of the dynamic properties of fine-grained concrete reinforced with fine-meshed meshes under dynamic uniaxial compression relative to the original fine-grained concrete has been carried out. Reinforced samples were made by pouring concrete into molds with pre-installed mesh frames. Dynamic tests have been carried out. Dynamic compression tests were carried out using the Kolsky method at strain rates from 30 to 600 s^{-1}. The paper presents the composition of the test material, test parameters, as well as a comparative analysis of the data obtained. The introduction of reinforcing meshes into the original fine-grained concrete increased the dynamic strength of the material. The dependences obtained demonstrate that the maximum breaking stresses achieved in the experiments increase linearly with the growth of the strain rate, as do the corresponding limiting strains. The time before the onset of fracture decreases with increasing strain rate according to a power law.

Key words: Dynamic strength · Stress · Strain · Strain rate · Concrete · Reinforced concrete · Dynamic tests · Kolsky method · Experiment

18.1 Introduction

The relevance of the study is due to the fact that in parallel with the growth of the technogenicity of our civilization, the number of emergency situations is growing, exposing the structures of buildings and structures for civil, industrial or military purposes to high-speed dynamic effects in the form of shocks and explosions. In

---

Mikhail E. Gonov · Vladimir V. Balandin · Anatoly M. Bragov · Aleksandr Yu. Konstantinov
National Research Lobachevsky State University of Nizhny Novgorod, 23 Gagarin Avenue, Nizhny Novgorod 603022, Russian Federation,
e-mail: gonov_mikhail@mech.unn.ru, bragov@mech.unn.ru, rustydog2007@yandex.ru, constantinov.al@yandex.ru

H. Altenbach et al. (eds.), *Sixty Shades of Generalized Continua*,
Advanced Structured Materials 170, https://doi.org/10.1007/978-3-031-26186-2_18

addition to man-made disasters, the increasing frequency of natural disasters, as well as the increased terrorist threat in the form of various explosive and combustible substances, are coming to the fore. The main danger of such phenomena is the loss of human lives, both with the loss of the bearing capacity of buildings and structures, and with the occurrence of many injuries from fragments of fragile materials formed during their dynamic destruction. Since concrete is currently one of the most common building materials, a key method to increase its strength is the addition of finely dispersed reinforcement: fiber reinforcement and fine mesh.

The practical applicability of the obtained results is related to the field of three-dimensional computer modeling, in which the behavior of real materials and structures under the action of normal or extreme (emergency) loads is re-placed by their mathematical model, which requires various experimental data obtained in the articles, a lot of parameters and constants. Ordinary concrete has relatively low tensile strength and low ductility, so it is prone to cracking. The formation of cracks leads to the early onset of the destruction of concrete or rein-forced concrete. It has been proven that fine-mesh reinforcement increases the tensile strength and plasticity of concrete [1]-[5]. We note right away that there are much fewer studies of the dynamic properties of fine-grained concretes rein-forced with meshes with a small cell size (up to 10 mm) than fine-grained concretes reinforced with fiber.

In [6] a new environmentally friendly building material is presented - high-performance geopolymer concrete. Both numerical and experimental studies have been carried out on a new type of structural plates reinforced with steel wire mesh for protection against explosions near the ground surface. To compare the results, conventional concrete slabs reinforced with steel reinforcement and subjected to explosive loading were also investigated. An experimental study was carried out to study the mechanism of slab damage. It was found that a geopolymer concrete slab reinforced with steel wire mesh showed less damage when exposed to 50 kg of trinitrotoluene (TNT) at distances of 3 m, 5 m and 7 m compared to a concrete slab. Numerical analysis was then carried out to further study the dynamic characteristics of the slab. The combination of steel wire mesh reinforcement with geopolymer concrete can help improve blast resistance, resulting in a promising and environmentally friendly structural protective material.

It was noted in [7] that the use of high-strength fiber-reinforced concrete in practical construction is very expensive due to the high content of steel fibers (> 2.5% by volume). The study proposes two column designs (2000 × 168 × 168 mm). Hollow core components and steel wire mesh reinforced components were cast from high-strength concrete containing 1.5% steel fiber by volume, and the impact resistance of both types of structures was also studied. The test pieces included two hollow core square and round hollow core columns and two steel wire mesh reinforced columns with 6 and 10 layers of wire reinforcement. The impact scenario was simulated using a 411 kg jackhammer freely falling from a height of 1.25 m to the middle of the span of the test specimen. The results showed that all specimens retained flexural strength with minimal damage. The developed numerical model recorded the impact force, structural deformation and damage with sufficient accuracy. Using the tested model, the distribution of dynamic shear and moment, the level of damage to the columns after the impact were evaluated. The influence of the shape and ratio of hollow sections, the level of axial load and the coefficient of longitudinal reinforcement for columns with a hollow core, as well as the influence of layers of steel wire mesh for columns reinforced with steel wire mesh, was investigated. Compared to other hollow columns at impact velocities from 4.95 m/s to 6.64 m/s, round hollow columns with a 15% cavity ratio proved to be the most effective in terms of cost and impact resistance. A column reinforced with steel wire mesh, reinforced in the entire section, has better impact resistance than its column, which had wire mesh reinforcement only in the tension zone.

In [8] experimental and numerical studies of the impact resistance of targets made of reactive powder concrete (RPC) reinforced with 44-layer steel wire meshes are presented. Steel projectiles with an average mass of 330 g and striking speeds from 550 m/s to 800 m/s were fired at RPC cylindrical targets with a diameter of 750 mm and a thickness of 700 mm. The results showed that the helical distribution of the steel wire mesh reinforcement in the RPC, perpendicular to projectile penetration, can effectively reflect and refract the stress wave generated by projectile impact, resulting in better impact resistance relative to projectile penetration. Steel wire mesh reinforcement in RPC targets effectively improves impact resistance and reduces crater diameter compared to the previous target study. The results of the experiment show that with an in-crease in the impact velocity of the projectile, the diameter of the crater increases.

In [9], an increase in electromagnetic protection and impact resistance of reinforced concrete walls of protective structures was considered. Electromagnetic interference shielding has received attention in the design of radiation reduction processes to protect people or equipment. Several studies have examined the use of hybrid amplification techniques for shielding effectiveness or examined the relationship between damaged areas and shielding effectiveness. In the work, a rein-forced concrete (RC) wall was prepared, subjected to various impact loads, containing steel fiber, metal mesh - mesh reinforcement and hybrid reinforcement. Compared to the 300 mm thick RC specimens and the same type reinforced specimens, the hybrid reinforced specimens had about 25.9 times and 2.4 times higher shielding efficiency, respectively. Samples reinforced with metal mesh showed a free area ratio of less than 150% and a shielding efficiency of more than 30 dB. Hybrid metal mesh and optional metal mesh have reached more than 40db. The hybrid reinforced specimens have demonstrated improved impact resistance and high shielding performance in damaged conditions.

In [10], a comparative evaluation of steel wire mesh, steel fiber and high-strength concrete slabs reinforced with polyethylene fiber was carried out during explosion tests. Due to the relatively low tensile strength, concrete tends to tensile failure and crack under external loads. To improve the tensile strength and ductility of the concrete material, the study considered possible solutions, including fiber reinforcement and steel mesh reinforcement. Ultra high molecular weight polyethylene fiber and steel wire meshes were mixed at different volume fractions in a concrete matrix. Static testing of reinforced concrete slab materials, including uniaxial compression and bending tests, showed that the addition of steel fiber resulted in a better increase in strength, while ultra high molecular weight polyethylene fiber provided better material ductility. Concrete samples with hybrid steel fiber reinforcement and steel mesh showed high strength and ductility. Field blast tests are designed to study the behavior of blasts at close range. Explosion tests show different damage profiles. The results showed the benefits of replacing the steel fiber with ultra-high molecular weight polyethylene or steel wire mesh.

18.2 Test Method

High-speed tests under conditions of a one-dimensional compressive stress state were carried out on an experimental setup SHPB-60 [11]-[13], the scheme of which is shown in Fig. 18.1. The experimental setup according to the Kolsky method includes a system of measuring rods, between which a test sample is installed, a gas gun for accelerating a cylindrical impactor, strain gauges, a velocity meter, recording and computing equipment with a software package. Measuring rods, both loading and supporting, as well as a cylindrical striker, are made of D16T duralumin alloy. The striker length in all experiments was 300 mm. The amplitude of the loading wave and, accordingly, the value of the realized strain rate were varied by changing the impactor velocity. The loading modes were chosen in such a way that a gradual increase in the strain rate was observed. In one of the rods, after the impact of the impactor, a one-dimensional elastic compression wave is excited, which propagates along the rods at the speed of sound. Upon reaching the sample, this wave splits due to the difference in the acoustic stiffness of the materials of the rod and the sample, as well

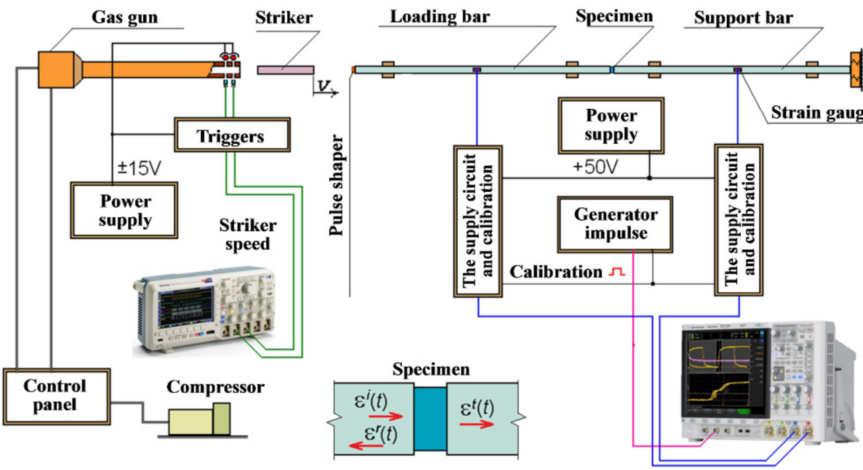

Fig. 18.1: Scheme of the installation for testing under compression in the condition of a uniaxial stress state.

as the areas of their cross sections: part of it is reflected back by a tension wave, and part passes through the sample into the second rod by a compression wave. In this case, the sample undergoes elastic-plastic deformation or destruction, while the rods are deformed elastically. By registering elastic strain pulses in measuring rods with strain gauges according to the formulas proposed for the first time by Kolsky, it is possible to determine the stresses, strains, and strain rates in the sample as a function of time.

To fulfill the main premise of the Kolsky method - a uniaxial stress state in the sample, the main recommendations were taken into account, namely: the ratio of the length of the sample to the diameter within 0.3 - 1.0; treatment of the ends of the measuring rods before the start of each experiment with Litol lubricant to reduce the effect of friction forces during the radial expansion of the sample.

18.3 Characteristics of the Tested Materials

This section presents the results of tests of reinforced fine-grained concrete of class B25, made by pouring concrete into molds in which mesh frames were previously installed (Fig. 18.2). Reinforcing fine-mesh mesh is made of light O/N wire in accordance with GOST 3282-74 from steel grade 1PS, mesh size 10x10 mm, wire

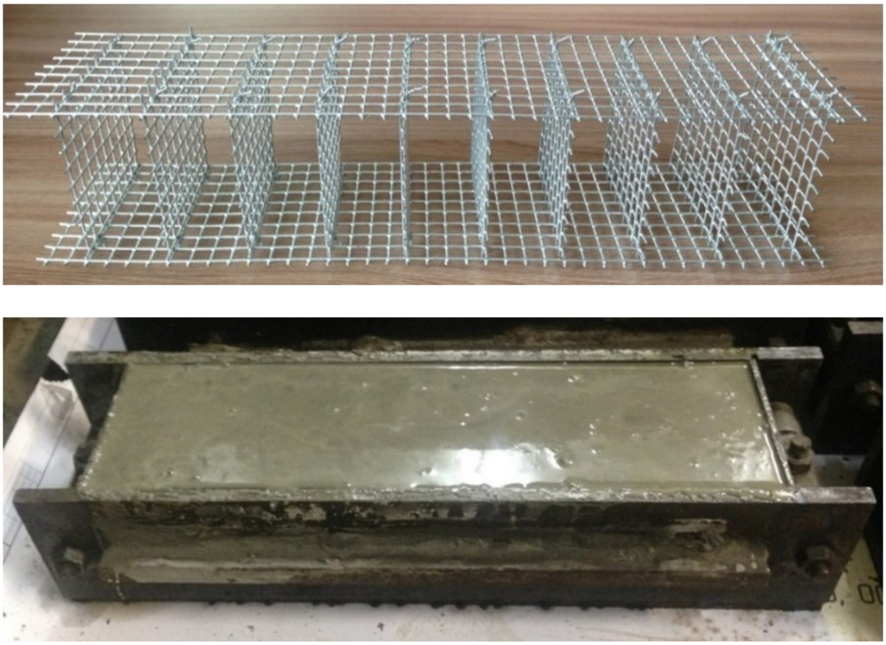

Fig. 18.2: Reinforcing mesh frame and poured concrete blank.

thickness 1.4 mm. The composition of fine-grained concrete is presented in Table 18.1.

After keeping the manufactured reinforced beams until the standard strength was reached, samples were made from it. Using a Hilti DD130 drilling rig, cores with a diameter of ~54 mm were drilled from the beam, which were then cut into individual reinforced samples ~30 mm thick using a Cedima CTS-57-G stone-cutting machine (Fig. 18.3).

18.4 Results of Dynamic Tests for Uniaxial Compression

High-speed tests under conditions of one-dimensional stress state in compression were carried out on the experimental setup SHPB-60, on samples with a diameter of 53 mm and a length of 30 mm. Reinforced concrete was tested at four different speed modes, 2-4 shots for each mode. The strain rates were in the range from 30 to 600 s^{-1}. Test parameters are shown in Table 18.2.

Below is a set of dependences of stress change and strain rate for each mode in the form of averaged dependences with a confidence interval. The initial sections of the resulting deformation diagrams are linear, and the fall-ing branches of the diagrams and examination of the samples indicate that the samples were destroyed during the experiment, which is confirmed by the photo-graphs of the destroyed samples in Fig. 18.4.

Figure 18.5 shows the averaged diagrams of the deformation of reinforced concrete with the chronology of the change in the strain rate. In Fig. 18.5, the straight line shows the dependence on stress, the dotted line shows the dependence on strain rate.

In the above diagrams, in the stress–strain axes $\sigma(\varepsilon)$, in the initial section of loading, one can distinguish a section where the growth of stress and strain occurs according to a law close to linear, and with further deformation, when the limiting stress values are reached, the concrete is intensively destroyed (in modes 2, 3, 4), which is accompanied by a decrease in stresses and an increase in deformations. For each of the resulting diagrams, characteristic points with the maximum achieved stresses ($\sigma_{\max}$) were identified, after which the destruction of the samples began. For these points, the corresponding values of ultimate strains ($\varepsilon_{\max}$) and time to failure ($\tau_{\max}$)

Table 18.1: The composition of fine-grained concrete class B25.

No.	Material	Consumption per 1 m^3 (kg)
1	Cement (grade D500)	480
2	Crushed stone (module 1-3 mm)	1250
3	Medium sand	390
4	Superplasticizer	2.4
5	Water	205

Fig. 18.3: Manufacture of reinforced concrete specimens.

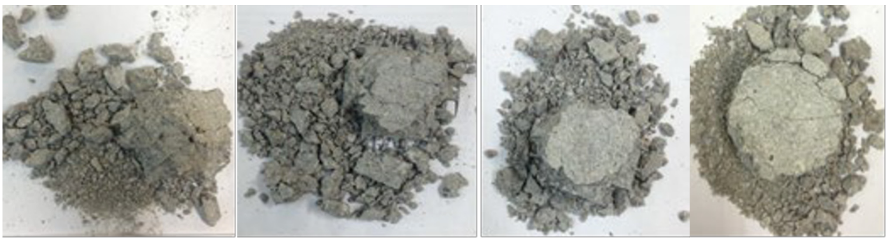

Specimen No. 3 Specimen No. 5 Specimen No. 7 Specimen No. 12

Fig. 18.4: The nature of the destruction of the specimens.

Table 18.2: Test parameters for reinforced concrete under dynamic compression.

Mode	Experiment Code	Loading parameters		Sample parameters			Experiment results				
		Pressure, bar	Striker speed, m/s	D, mm	$S_{c.s.}$, mm^2	L, mm	Ultimate stress, MPa	Ultimate strain, %	Strain rate, 1/s	Lifetime, ms	DIF
1	c669-01	0,5	7,14	53,7	2265	29,75	52,01	0,6	36,4	99	2,1
	c669-02	0,5	4,3	53,7	2265	29,2	23,00	0,5	43,5	108	0,9
2	c669-03	1	14,5	53,4	2240	30,4	98,57	1,9	165,1	98	3,9
	c669-04	1	15,5	53,4	2240	30,16	99,94	2,0	176,7	100	4,0
3	c669-05	2,5	19	52,73	2184	30,69	124,15	2,5	219,1	108	5,0
	c669-06	2,5	20,4	53,5	2248	30,3	105,41	2,5	319,5	65	4,2
	c669-07	2,5	22,2	53,4	2240	30,13	113,10	3,1	313,9	90	4,5
	c669-08	2,5	22,7	53,5	2248	31	103,06	2,7	329,0	82	4,1
4	c669-09	3	26,5	53,2	2223	30,85	124,52	3,4	390,9	92	5,0
	c669-10	3	28,4	53,8	2273	30,9	101,73	4,5	579,5	90	4,1
	c669-11	3	29	53,4	2240	31	100,54	3,5	595,1	78	4,0
	c669-12	3	25,5	54,2	2307	30,3	120,60	3,1	374,5	80	4,8

DIF - Dynamic increase factor

are determined. The strain rates ($\dot{\varepsilon}$) were taken to be maximum before the samples began to fail, since they change during deformation. Figure 18.6 shows the speed dependences of the main characteristics of reinforced concrete. The dependences obtained demonstrate that with an increase in the strain rate, the maximum stresses increase, the corresponding limiting strains also in-crease (according to a linear law), and the time to failure decreases according to a power law.

Figure 18.7 shows the dependence of the DIF on the strain rate. The DIF index in the obtained range of strain rates ~ 30–600 s^{-1} varies depending on the strain rate from 2.9 to 5.

18.5 Conclusion

An experimental study of the dynamic properties of fine-grained concrete rein-forced with steel fine-mesh mesh under uniaxial compression has been carried out. Diagrams of dynamic deformation at strain rates from 30 to 600 s^{-1} are obtained, the results of which determine the characteristics of strength and deformability, and determine the dependences on various strain rates.

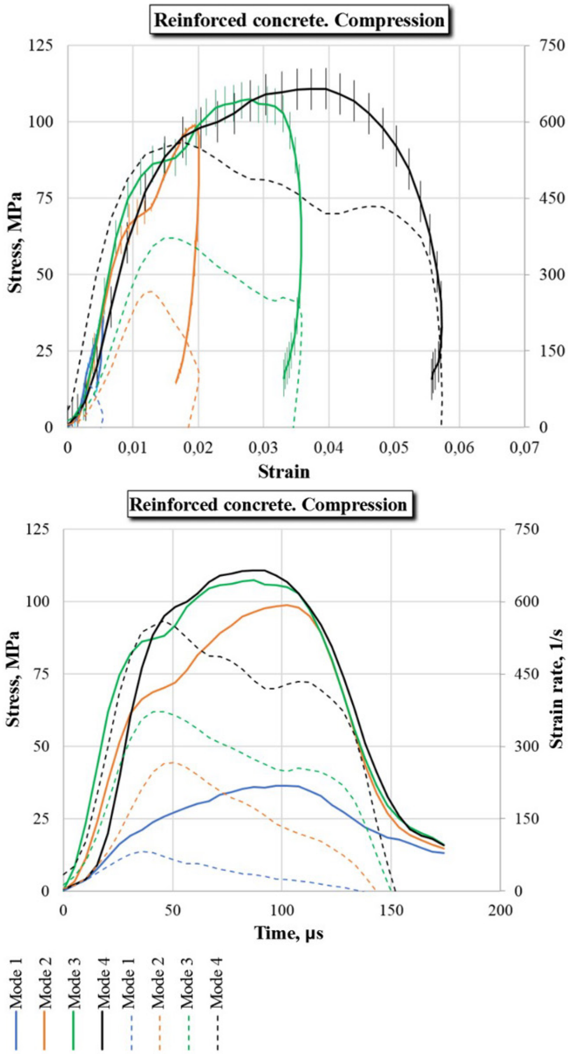

Fig. 18.5: Averaged diagrams $\sigma(\varepsilon)$ and $\dot{\varepsilon}(\varepsilon)$, $\sigma(t)$ and $\dot{\varepsilon}(t)$ under compression for all modes.

The introduction of a reinforcing fine-mesh mesh into the original fine-grained concrete increased the dynamic strength of the material at strain rates from 200 to 400 s^{-1} by an average of 45% relative to the previously tested fine-grained concrete [14]. The DIF values reached an average value of 4.0.

Acknowledgements The work was supported by the Russian Science Foundation grant No. 22-19-00138.

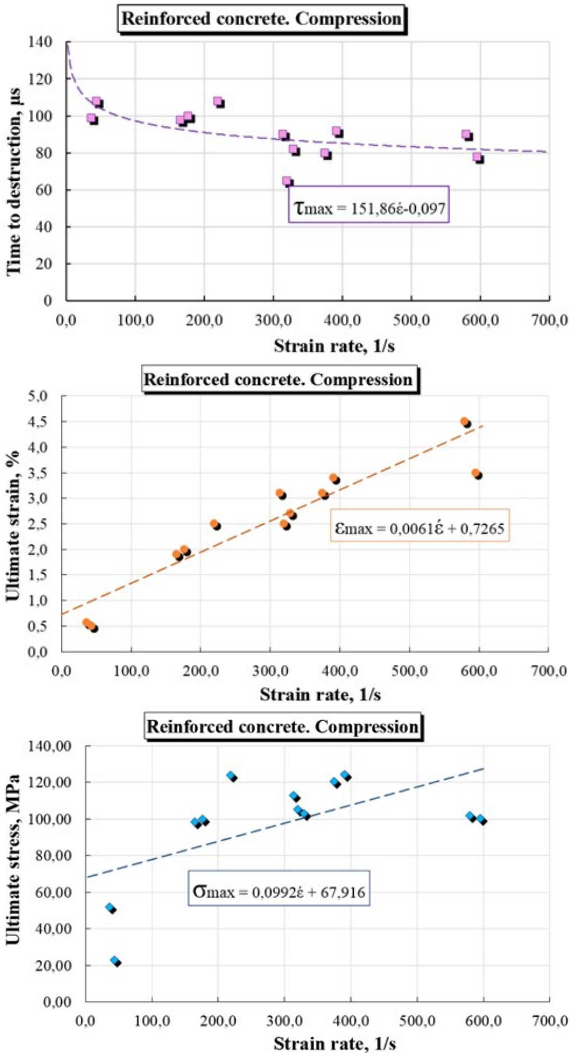

Fig. 18.6: Influence of strain rate on the mechanical properties of reinforced concrete under dynamic compression.

References

[1] Yu R, van Beers L, Spiesz P, Brouwers HJH (2016) Impact resistance of a sustainable Ultra-High Performance Fibre Reinforced Concrete (UHPFRC) under pendulum impact loadings, Construction and Building Materials **107**:203–215. DOI 10.1016/j.conbuildmat.2015.12.157

Fig. 18.7 Dependence of DIF on strain rate

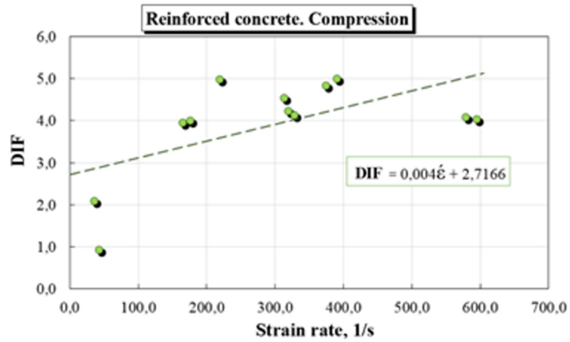

[2] Wang D, Shi C, Wu Z, Xiao J, Huang Z, Fang Z. (2015) A review on ultra high performance concrete: Part II. Hydration, microstructure and properties, Construction and Building Materials **96**:368–377. DOI 10.1016/j.conbuildmat.2015.08.095

[3] Li PP, Yu QL (2019) Responses and post-impact properties of ultra-high performance fibre reinforced concrete under pendulum impact, Composite Structures **208** (2019) 806–815. DOI 10.1016/j.compstruct.2018.10.071

[4] Li PP, Brouwers HJH, Yu Q (2020) Influence of key design parameters of ultra-high performance fibre reinforced concrete on in-service bullet resistance, International Journal of Impact Engineering **136**:103434. DOI 10.1016/j.ijimpeng.2019.103434

[5] Khosravani MR, Weinberg K (2018) A review on split Hopkinson bar experiments on the dynamic characterisation of concrete, Construction and Building Materials **190**:1264–1283. DOI 10.1016/j.conbuildmat.2018.09.187

[6] Meng Q, Wu C, Su Y, Li J, Liu J, Pang J (2019) A study of steel wire mesh reinforced high performance geopolymer concrete slabs under blast loading, Journal of Cleaner Production **210**:1150-1163. DOI 10.1016/j.jclepro.2018.11.083

[7] Wei J, Li J, Wu C (2020) Behaviour of hollow-core and steel wire mesh reinforced ultra-high performance concrete columns under lateral impact loading, International Journal of Impact Engineering **146**:103726. DOI 10.1016/j.ijimpeng.2020.103726

[8] Liu J., Wu C., Li J., Su Y., Shao R., Liu Z, Chen G (2017) Experimental and numerical study of reactive powder concrete reinforced with steel wire mesh against projectile penetration, International Journal of Impact Engineering **109**:131-149. DOI 10.1016/j.ijimpeng.2017.06.006

[9] Yuan T-F, Choi J-S, Hong S-H, Yoon Y-S (2021) Enhancing the electromagnetic shielding and impact resistance of a reinforced concrete wall for protective structures, Cement and Concrete Composites **122**:104148. DOI 10.1016/j.cemconcomp.2021.104148

[10] Li J, Wu C, Liu Z-X (2018) Comparative evaluation of steel wire mesh, steel fibre and high performance polyethylene fibre reinforced concrete slabs in blast tests, Thin-Walled Structures **126**:117-126. DOI 10.1016/j.tws.2017.05.023

[11] Bragov AM, Igumnov LA, Lomunov AK (2015) High-Speed Deformation of Fine-Grained Concrete and Fiber-Reinforced Concrete (in Russ.), N. Novgorod: Nizhny Novgorod State University Publishing House

[12] Bragov AM, Konstantinov AY, Lamzin DA, Lomunov AK, Karihaloo BL, Petrov YV, Smirnov IV (2012) High-rate deformation and fracture of fiber reinforced concrete, Journal of Applied Mechanics and Technical Physics **53**(6):926–933. DOI 10.1134/S0021894412060168

[13] Bragov AM, Gonov ME, Lomunov AK (2019) Experimental study of the dynamic properties of concrete under compressive load, International Conference on Nonlinear Solid Mechanics ICoNSoM2019 June 16-19, 2019, pp 403-412.

[14] Bragov AM, Gonov ME, Lamzin DA, Lomunov AK, Modin IA (2021) Response of fine-grained fiber-reinforced concretes under dynamic compression, Materials Physics and Mechanics **47**(6):962-967. DOI 10.18149/MPM.4762021_14